Influence of laser parameters and experimental conditions on nonphotochemical laser-induced nucleation of glycine polymorphs

Irimia, Daniel; Shirley, Jenkins Jose; Garg, Anshul S.; Nijland, Davey P.A.; van der Heijden, Antoine E.D.M.; Kramer, Herman J.M.; Eral, Huseyin Burak

DOI
10.1021/acs.cgd.0c01415

Publication date
2021

Document Version
Final published version

Published in
Crystal Growth and Design

Citation (APA)
Irimia, D., Shirley, J. J., Garg, A. S., Nijland, D. P. A., van der Heijden, A. E. D. M., Kramer, H. J. M., & Eral, H. B. (2021). Influence of laser parameters and experimental conditions on nonphotochemical laser-induced nucleation of glycine polymorphs. *Crystal Growth and Design*, *21*(1), 631−641. https://doi.org/10.1021/acs.cgd.0c01415

CRYSTAL GROWTH & DESIGN

pubs.acs.org/crystal

Article

Influence of Laser Parameters and Experimental Conditions on Nonphotochemical Laser-Induced Nucleation of Glycine Polymorphs

Daniel Irimia, Jenkins Jose Shirley, Anshul S. Garg, Davey P.A. Nijland, Antoine E. D. M. van der Heijden, Herman J. M. Kramer, and Huseyin Burak Eral*

Cite This: *Cryst. Growth Des.* 2021, 21, 631−641

Read Online

ACCESS | Metrics & More | Article Recommendations | Supporting Information

ABSTRACT: Nonphotochemical laser-induced nucleation (NPLIN) is a promising primary nucleation control method, yet its underlying mechanism remains elusive. To contribute to the discussion on whether the polarization of laser irradiation in NPLIN experiments influences the polymorphic outcome, we revisit NPLIN experiments with aqueous glycine solutions with supersaturations ranging between S = 1.5 and S = 1.7 irradiated by nanosecond pulses (∼7 ns) of near-infrared wavelength (1064 nm). Systematically altering laser light excitation properties, including the number of pulses and type of polarization, we quantified the nucleation kinetics and characterized the polymorphic form that crystallized upon laser irradiation. Due to the stochasticity of the nucleation process, a large number of samples (>100 per each experimental point) were studied under carefully controlled experimental conditions such as the ambient temperature, cooling rate, and aging period. We observed significant differences among laser-irradiated, spontaneously nucleated, and crash-cooled samples in terms of nucleation kinetics and polymorphic form. This result indicates that laser irradiation provides a different polymorph-forming pathway in comparison to crash-cooling and spontaneous nucleation. However, no clear dependence between the polymorphic form and the polarization of laser irradiation is observed. We discuss our results in the context of previous reports supported thorough quantification of sample heating in NPLIN experiments.

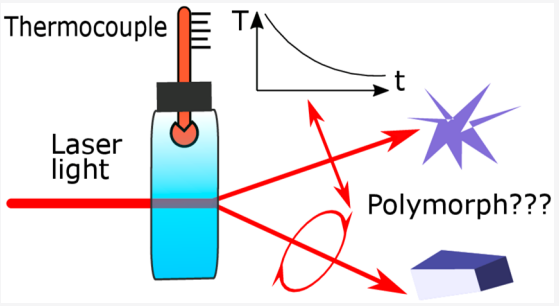

INTRODUCTION

Nonpotochemical laser-induced nucleation, usually referred to as NPLIN, is a term that was coined more than two decades ago by Garetz et al., who were investigating the nonlinear optical properties (second harmonic generation) of supersaturated aqueous urea solutions.[1] Garetz et al. serendipitously discovered that laser radiation induced crystallization of urea from solution at nucleation rates far beyond those of undisturbed samples. This light−matter interaction process was concluded to be nonphotochemical, since both the solute and solution were transparent to the laser wavelength used in the experiment. This finding garnered significant scientific interest in the field of primary nucleation control, and laser-induced nucleation emerged as a promising alternative to the traditional techniques, including spontaneous nucleation and seeding techniques, or more intrusive methods such as sonocrystallization[2,3] and microwave-assisted nucleation.[4−6]

Since then, a considerable number of studies have been reported with various types of chemical compounds and by employing an array of laser systems whose properties/parameters including time duration (continuous, femtosecond, picosecond, nanosecond regime),[7−10] field polarization (linear, circular and elliptical),[11−13] wavelength (UV−vis−IR),[14] or intensity (ionizing, nonionizing),[15−17] were altered to control primary nucleation. However, despite the remarkable scientific progress, the underlying mechanism behind the laser-induced nucleation still remains unclear. Several possible mechanisms, such as the optical Kerr effect (OKE), dielectric polarization, shock waves, and cavitation and nanoparticle heating, have been proposed in the literature.[18] We currently do not have sufficiently conclusive agreement between the experimental observations and the predictions of the proposed mechanisms to completely validate or invalidate each mechanism. Each of the aforementioned mechanisms appears to describe reasonably the nucleation in some systems but fails in others. For example, OKE is used to explain the nucleation of chemical systems possessing anisotropic electronic polarizability whose free energy barrier is reduced through laser-induced molecular alignment.[19] However, the field strengths required to create a significant alignment of small molecules was found to be much higher in Monte Carlo simulations of a Potts lattice gas model[20] in comparison to those employed in the NPLIN experiments. Dielectric polarization is recalled to explain the

Received: October 21, 2020
Revised: December 9, 2020
Published: December 22, 2020

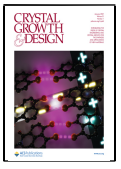

https://dx.doi.org/10.1021/acs.cgd.0c01415
Cryst. Growth Des. 2021, 21, 631−641

nucleation of compounds with cubic crystal symmetry such as the common halide salts.[16,21,22] The mechanism relies on the ability of the laser fields to lower the free energy barrier by polarizing the electrons of atoms in solutions where the relative permittivity of the solute, ε_p, is larger than that of the solution, ε_s. The notable downside of the dielectric polarization model is that the free energy barrier is not reduced significantly at "nonphotochemical" field strengths, just as in the case of OKE. Shock waves and cavitation are also observed to induce crystallization in aqueous solutions at laser fluxes higher than those in NPLIN experiments.[23−25] Hence, these observations along with a large body of literature on laser-induced cavitation and bubble formation in single-component systems[26] triggered researchers to speculate on how cavitation and shock waves can play a role in NPLIN studies.[18] Moreover, cavitation and shock waves can be generated by other methods, such as mechanical disturbances and ultrasound in addition to laser light. The light-based mechanisms involve two nucleation routes: laser-induced cavitation and laser-induced pressure waves. However, in both cases focused laser beams of high intensities above the NPLIN level are required to observe large enough cavitation bubbles (above the diffraction limit). Nanoparticle heating has been proposed as an explanation on how cavitation can occur at NPLIN intensities.[27−29] In this mechanism, the absorption of light photons by impurities present in the exposed solution causes local heating to several hundreds or thousands of kelvin, generating vapor cavities, causing concentration gradients, and triggering nucleation. Nanoparticle absorption of laser light could explain the results from numerous NPLIN experiments including this study, but the main burden lies in identifying the role of impurity particles and their chemical nature.[30] So far, Ward et al. have successfully identified the nature and size of impurities in aqueous ammonium chloride solutions.[31]

Among a substantial group of organic and inorganic chemical compounds, including sodium chloride, ammonium chloride, urea, histidine, and hen-egg-white-lysozyme (HEWL), glycine appeared as a molecular system of paramount importance for the exploration of nonphotochemical laser-induced nucleation. It is the simplest amino acid and is a common building block of proteins in living organisms. Glycine exhibits six polymorphic forms, three of which (α, β, γ) can be crystallized at ambient pressure and temperature. The relative stabilities of the three forms are $\beta < \alpha < \gamma$. While γ-glycine is the most thermodynamically stable polymorph, α-glycine is observed as the main polymorph, crystallizing spontaneously under almost any experimental conditions from pure aqueous solutions.[32] Due to these well-studied polymorphs, glycine has been used as a benchmark molecule for a number of studies investigating the control of polymorphism.

Controlling crystal polymorphism is of great interest to the pharmaceutical sector due to an intimate relationship between solubility and polymorphism. Polymorphism also affects physical parameters such as hardness and aspect ratio of crystals, both of which being significant to the pharmaceutical industry: e.g., for ease in making tablets. Different polymorphs of the same compound can have significantly different solubilities, and hence controlling the polymorphic form can drastically influence the bioavailability. Such applications have increased the awareness of and interest in polymorphism over the past century, with various approaches being developed in efforts to control polymorphism during the crystallization process.[33,34] Traditional approaches for polymorph control include the seeding of solutions with crystallites of the desired polymorph and the use of soluble additives that can inhibit or promote the growth of a particular polymorph.[35,36] Meanwhile, NPLIN has also been proposed as a promising tool to dictate the crystal structure using the properties of laser light.[37]

Garetz et al. were the first to report a polarization switching window in which the formation of a particular polymorph of glycine depends on the polarization state of the laser light being used.[12] Their results were reproduced a couple of years later,[13] but no other independent study on glycine was able to confirm the original findings. In addition, Liu et al. reported conflicting results, as they observed no dependence of glycine's polymorphic forms on laser polarization.[38] However, various studies successfully demonstrated the role of laser polarization in controlling polymorphism also in other chemical compounds, including carbamazepine,[39] L-histidine,[40] and sulfathiazole.[41] To sum up, this interesting collection of contradicting experimental evidence calls for revisiting NPLIN experiments where the polarization switching effect, i.e. the ability of the laser polarization to manipulate polymorphism crystallizing from solution, is rigorously investigated. As the nucleation process is highly stochastic and is strongly influenced by the experimental conditions, a consistent set of experimental results with a statistically significant number of samples is mandatory.

The goal of the current work is to investigate the effect of nanosecond light pulses on the nucleation kinetics and polymorphic form of glycine crystallized from solution using a statistically significant number of samples (>100 samples per experimental parameter). To contribute to the discussion on polarization switching, the investigation systematically considers the laser light excitation properties (number of pulses, type of polarization, wavelength, and energy density) under carefully controlled experimental conditions such as ambient temperature, cooling rate, and aging period. Supersaturated solutions exposed to laser irradiation with canonical NPLIN parameters (exposure to a single pulse of linearly polarized light at 1064 nm) showed significantly faster nucleation kinetics and produced different polymorphs in comparison to spontaneously nucleated[42] and crash-cooled samples used in this study at the same supersaturation. This result indicates that laser irradiation provides a different polymorph-forming pathway in comparison to crash-cooling and spontaneous nucleation. However, irradiation with circularly and linearly polarized light facilitated crystallization of the same polymorph across all supersaturations covered in this study. This result is in accordance with the results of Liu et al.[38] but different from those of Garetz and co-workers.[12,13] To shed light on the origin of this variation, we quantified the energy losses by reflection of the laser beam at the air−glass and glass−sample interfaces within the experimental system (the solution and the glass vial) by carefully measuring the energy at different wavelengths before and after the sample vials. Furthermore, the absorption of energy by the solution has been measured by using various approaches in relation to sample heating. We discuss our results using the thorough quantification of energy losses and sample heating in NPLIN experiments.

EXPERIMENTAL METHODS AND LAYOUT

Glycine (Sigma-Aldrich, 33226, puriss p.a., buffer substance, 99.7−101%) was used without any additional purification and dissolved in ultrapure water (Elga Purelab Ultra, 18.2 MΩ cm) to prepare stock solutions at the supersaturations of interest. Glycine concentrations in

https://dx.doi.org/10.1021/acs.cgd.0c01415
Cryst. Growth Des. 2021, 21, 631−641

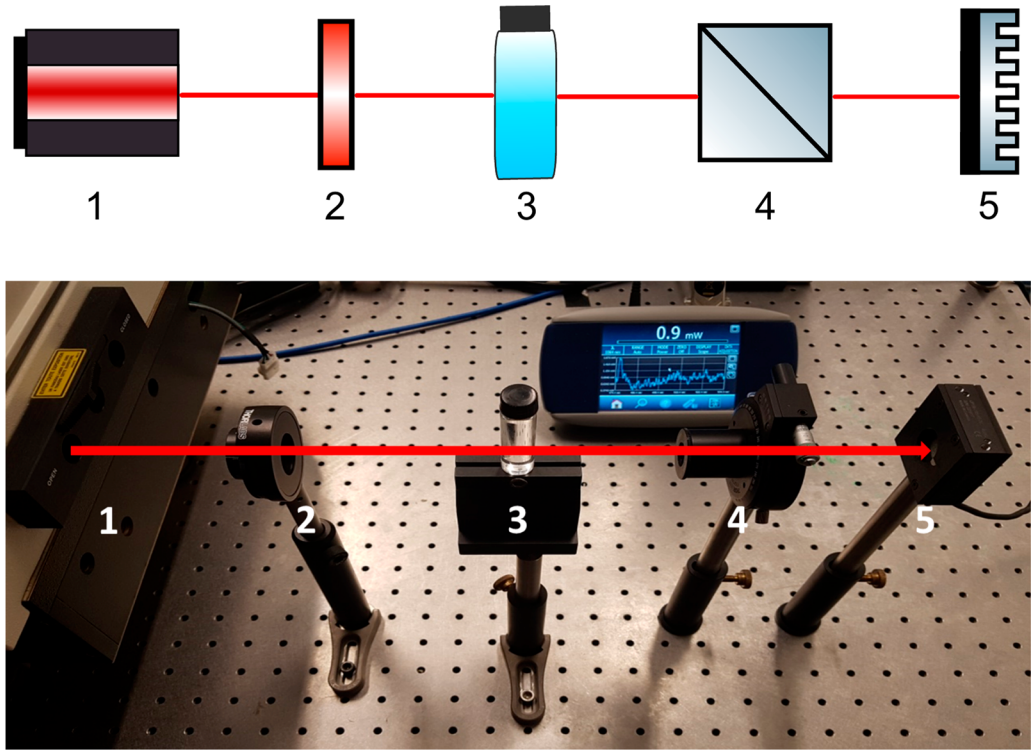

Figure 1. Schematic and photograph of the experimental layout: (1) Nd:YAG laser source; (2) quarter-wave plate at 1064 nm; (3) sample vial containing supersaturated aqueous glycine solution; (4) Glan-Laser polarizer; (5) energy meter.

the range of 367.5−416.5 g/kg water were used relative to the solubility of 245 g/kg water at 24 °C to attain supersaturations between 1.5 and 1.7. There are significant differences in the solubilities of glycine reported in the literature,[43−45] but in this work we referenced our supersaturations to the solubility of the α-glycine polymorph on the basis of a comprehensive data analysis performed by Liu et al.[38] Powder XRD analysis revealed that the polymorphic form of solid commercial glycine was α-type within the accuracy of this method.

The samples were prepared by transferring the stock solutions into small cylindrical borosilicate glass vials (BGB, volume 8 mL, dimensions 61 × 16.6 mm) sealed with screw caps featuring septa of silicone rubber/PTFE inserts. After the transfer, the sample vials were further kept in the oven at 65 °C to ensure the complete dissolution of glycine. After a few days, they were placed into a thermostated water bath, cooled gradually to 24 °C over the course of 1 day, and aged for at least 3 days. A few test batches of samples were at first maintained in the water bath for 1 week to account for spontaneous nucleation, which needed to be separated from the NPLIN process.

The schematic of the optical setup is depicted in Figure 1. The laser light source was a Q-switched Nd:YAG laser (Continuum Powerlite DLS 8000 model) capable of producing a train of 7 ns linearly polarized light pulses at a fundamental wavelength of 1064 nm, a repetition rate of 10 Hz, and an average power of 10 W (1 J/pulse). The 9 mm diameter beam featured a Gaussian spatial and temporal intensity distribution. Inside the sample, the beam was focused in the horizontal plane due to the curved shape of the glass vial, which acted as a cylindrical lens. Thus, the horizontal diameter of the laser spot was reduced to half its size at the exit of the sample vial, as shown in Figure S1 in the Supporting Information, and the optical power density was therefore doubled. On the basis of the above settings, we calculated the average linear power density of the laser beam to be 0.225 GW/cm^2 (input) and 0.450 GW/cm^2 (exit). However, these values must be corrected for losses due to reflection and absorption in the glass sample vials, which will be discussed in the Results and Discussion. The experiments described in the present work were performed using a larger beam diameter in order to enhance the nucleation fraction through a larger exposed volume (~0.705 cm^3) and a single pulse instead of 600 in order to minimize the heating effects caused by the water absorption at 1064 nm.

In addition to the near-infrared radiation, wavelengths of 532 and 355 nm, respectively, were also available via frequency doubling and tripling in KDP (potassium dihydrogen phosphate) nonlinear crystals. The power and energy measurements of the laser beam were performed by using a thermopile detector (type: UP19K-30H-VR-INT-D0) and a Gentec-EO Maestro energy meter. The time duration (fwhm) of the laser pulses was measured using a high-speed photodetector (Thorlabs Det10A 1 ns rise time) and visualized on a digital storage oscilloscope (Agilent InfiniiVision DSO-X 3054A). A zero-order quarter-wave plate was added into the beam path whenever the polarization of light was changed from linear to circular. A proper alignment of the quarter-wave plate, which was done with no sample in the laser path, ensured a constant power of the beam behind a Glan-Laser Calcite Polarizer (Eksma 440-2012-M2Ps) regardless of the orientation of its axis.

After irradiation, the samples were immediately returned to the temperature-controlled thermostat (24 °C) and provided a minimum waiting period of 7 h in order to detect the presence of crystals. The remaining vials that did not nucleate were further inspected at various time intervals within a range of up to 72 h. The glycine crystals were filtered out of solution, washed with deionized water, dried with compressed air, and crushed into powder using a mortar and pestle. This procedure is known to ensure the stability of glycine polymorphs during the sample analysis, as humidity, ambient gases, and the mechanical/grinding process were found to induce, under certain conditions, a phase transformation in crystalline glycine.[46] The powder was then placed inside a powder X-ray diffractometer (pXRD, Bruker D2 Phaser, Cu Kα_1 radiation λ = 1.5406 Å) to determine the form of polymorph attained in the NPLIN experiments.

Crash cooling from 65 to 24 °C was achieved by directly transferring the hot sample vials into the water bath of the cooling thermostat. Temperature profile measurements were performed using a batch of test samples at S = 1.7 and revealed that the samples

https://dx.doi.org/10.1021/acs.cgd.0c01415
Cryst. Growth Des. 2021, 21, 631−641

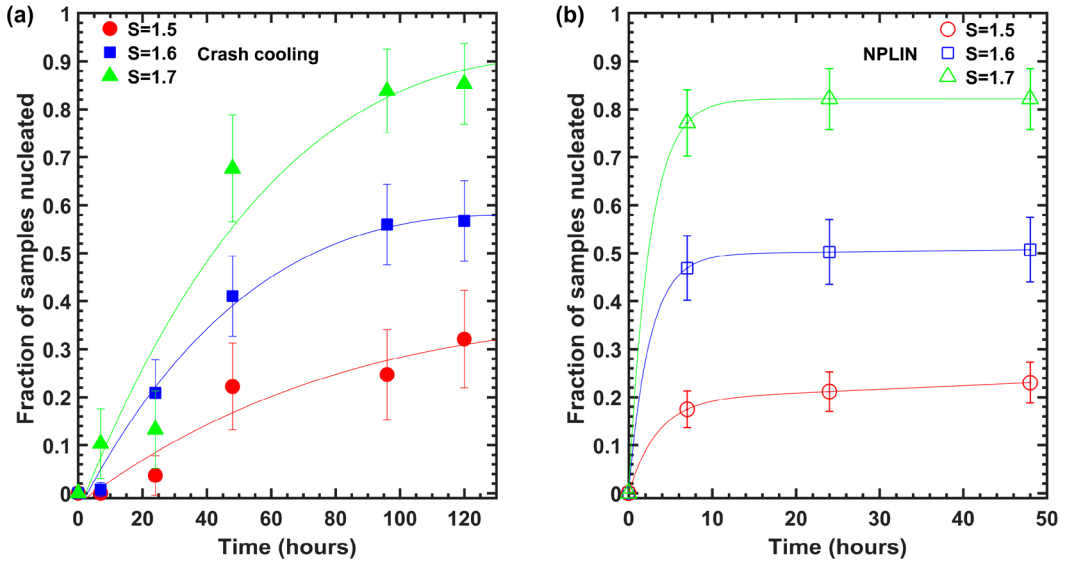

Figure 2. Plots of the fraction of nucleated samples at different supersaturations using crash-cooling (a) and NPLIN (b). Samples used for NPLIN were exposed to a single pulse (1 J) of linearly polarized light at 1064 nm. The solid curves are used as guide to the eye, and they do not necessarily cross the origin as shown. Error bars represent a 95% confidence interval calculated using the normal approximation method.

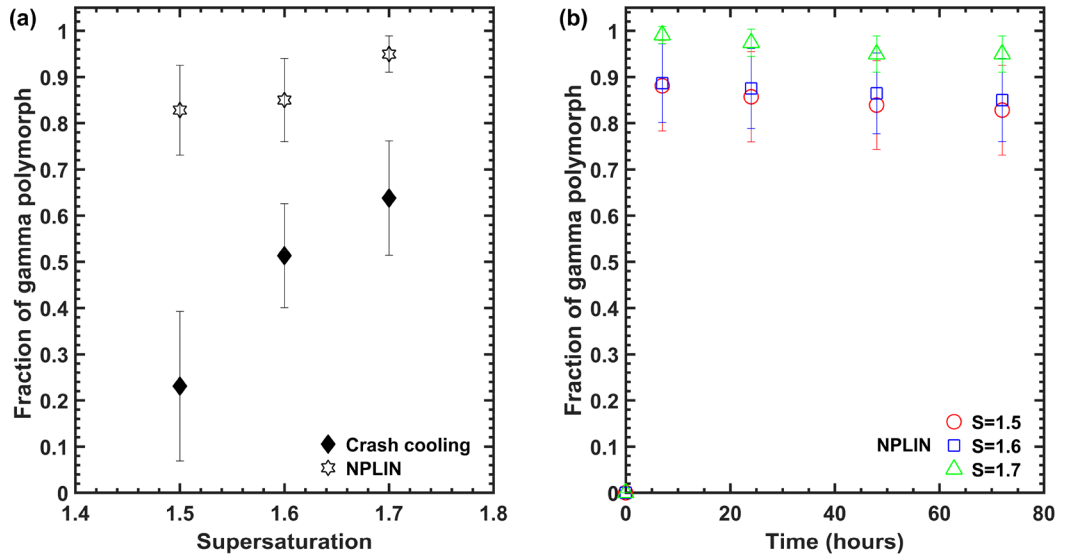

Figure 3. Plots of the fraction of γ-glycine samples nucleated versus supersaturation under crash-cooling and upon laser exposure with canonical NPLIN parameters: i.e., upon exposure to a single pulse (1 J) of linearly polarized light at 1064 nm, referred to as NPLIN in the legend. The fractions are reported 120 h after a temperature quench and 72 h after laser exposure as a function of the supersaturation (a). Time-dependent cumulative fraction of γ-glycine obtained via NPLIN as a function of time at three different supersaturations (b). Error bars in the data plots represent 95% confidence intervals obtained using the normal approximation method.

reached the target temperature within 5 min (see Figure S2 in the Supporting Information). The temperature was recorded using an eight-channel thermocouple data logger (Pico Technology USB TC-08) with the tip of the thermocouple (Type K) being inserted in the middle of the test sample.

RESULTS AND DISCUSSION

With the given experimental layout, the influence of laser parameters, the polarization of light (linear vs circular), and the number of pulses (1 vs 600), on nucleation kinetics and polymorphic form was studied. The effects of these parameters on the nucleation were tested at different supersaturations and compared with a control case of crash-cooling at each supersaturation. Figure 2 provides a comparison of the nucleation kinetics of glycine solutions crystallizing at three different supersaturations under crash-cooling and NPLIN conditions. A total number of 729 samples were used for NPLIN and 283 for the crash cooling (see Tables S1 and S2 in the Supporting Information for the distribution of samples among the three different supersaturations). All of the data plots contain error bars with a 95% confidence level.

The induction time for the crash-cooling experiments was monitored for 5 days, and the cumulative probability distribution is plotted in Figure 2a, which shows that glycine crystallizes rather slowly and has a long induction time. The solid curves are used as guide to the eye. It is important to emphasize that they do not necessarily cross the origin as shown, as we do not have measurements at small t. The transients in Figure 2b show the fraction of samples nucleated

https://dx.doi.org/10.1021/acs.cgd.0c01415
Cryst. Growth Des. 2021, 21, 631−641

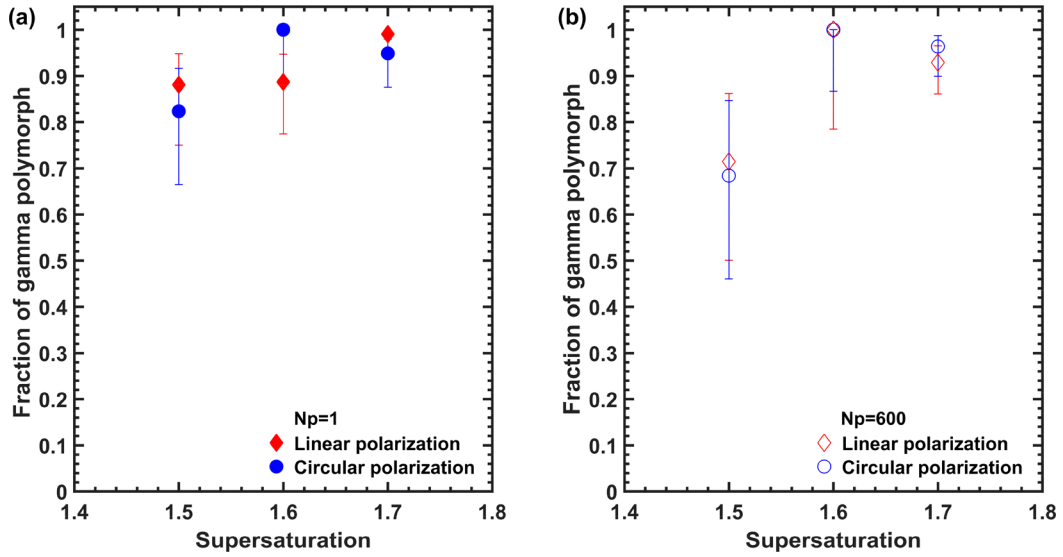

Figure 4. Fraction of γ-glycine formed 7 h after exposure to 1 J linearly and circularly polarized laser light at 1064 nm using a single pulse (a) and 600 pulses (b). The polarization-switching effect was not observed, as both linearly and circularly polarized light produce comparable fractions of γ-glycine regardless of the number of laser pulses used. Error bars in data plots represent 95% confidence intervals calculated using the Wilson score method.

using a single pulse of near-infrared linearly polarized light. It can be seen that, in comparison to crash cooling, laser irradiation significantly reduces the induction time regardless of the supersaturation of the solutions. On the basis of this observation, we deduce that laser exposure dominates the nucleation kinetics in the first 10 h after exposure, as seen in Figure 2b. In some cases this fast nucleation is followed by a much slower nucleation illustrated by a slight, slow increase in the nucleation probability, for instance for S = 1.5, which we attribute to spontaneous nucleation. The nucleation probabilities presented in this work are somewhat lower than the results of Sun et al.,[13] Liu et al.[38] and Javid et al.,[42] whose investigations showed that the fractions nucleated are considerable, even at supersaturation values below S = 1.5 (Figure 1a of ref 29). Although the laser intensity, wavelength, and ambient temperature were nearly similar to those in the previous studies on glycine, our samples were exposed to a single laser pulse of Gaussian spatial profile instead of the more common irradiation to a 600 pulse train of either Gaussian or near top-hat profile. In addition, the exposed volume of solution in our samples is at least 15-fold greater than those employed in other studies and our results originate from a larger number of samples per experimental set used. For each set of experimental conditions studying the laser-induced nucleation fraction at supersaturations between 1.5 and 1.7, we used between 140 and 378 samples, in comparison to Sun et al., who used a range of 40−90 samples, Liu et al., who used 12−98 samples, and Javid et al., who used ∼50−63 samples.

The fraction of samples that nucleated as γ-glycine under both crash-cooling and canonical NPLIN conditions at different supersaturations is shown in Figure 3. The investigation of polymorphism involved 283 samples for crash-cooling and 463 samples for NPLIN (Table S3 and S4 in the Supporting Information). Just like other nucleation methods such as sonocrystallization and nucleation by mechanical shock,[38] crash-cooling favors the formation of the γ-polymorph at higher supersaturations, as shown in Figure 3a. However, the NPLIN experiments reveal that already at lower supersaturations the γ-polymorph predominantly nucleates, approaching 100% at S = 1.7, showing that laser radiation is more effective and selective in separating the two polymorphic forms of glycine in aqueous solutions.

Figure 3b shows the fraction of nucleated samples that generated γ-glycine under canonical NPLIN conditions as a function of time after exposure. The fraction of the γ-polymorph, which is relatively high (above 80%) at all supersaturations, decreases slowly with time due to nucleation of additional samples that produce α-glycine. We attribute this to spontaneous nucleation. This observation was confirmed also by Javid et al.,[42] who reported that nucleation at longer times is spontaneous and yields mostly α-glycine.

As reported by Garetz and co-workers, a polarization-switching window in which the polarization state of laser light can bias the nucleation of a specific polymorphic form spans between supersaturations of 1.45 and 1.55. We attempted to reproduce their observations by exposing supersaturated solutions to both single (Figure 4a) and multiple (600) light pulses (Figure 4b) of linear and circular polarization. The results shown in Figure 4 are based on data given in Table S5 and reveal that such a window in which the polarization of the laser beam can be used to control the formation of either the α- or the γ-polymorph was not observed in our case.

Sun et al.[13] created a series of supersaturations by controlling the temperature within a temperature interval of 15−25 °C with a switching effect being clearly observed somewhere between 17 and 24 °C. Our experiments were performed at 24 °C, which lies at the upper limit of the temperature range where the binary polarization switching of glycine polymorphs was reported. By comparing parts a and b of Figure 4, one can observe that the results are nearly independent of the number of pulses and the type of polarization used. In addition, we conducted a round of tests for polarization switching in the middle of the supersaturation and temperature windows (S = 1.5 and T = 20 °C). We exposed 133 samples to single pulses of 0.45 GW/cm^2 in intensity, but the nucleation probability at this temperature was very low (1.5%) and thus inconclusive for the observation of the polarization-switching effect. Liu et al. performed similar

https://dx.doi.org/10.1021/acs.cgd.0c01415
Cryst. Growth Des. 2021, 21, 631−641

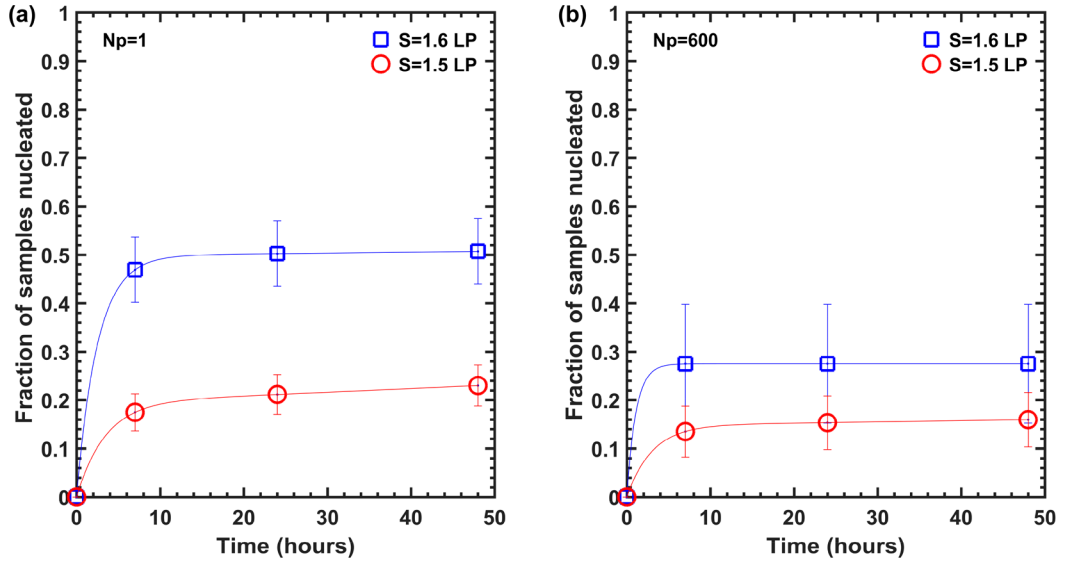

Figure 5. Plots of the fraction of glycine samples nucleated versus time. The results represent the cumulative nucleation fractions obtained at two different supersaturations and induced by 1-Joule linearly polarized light at 1064 nm: (a) samples exposed to 1 pulse; (b) samples exposed to 600 pulses. The solid curves are used as a guide to the eye, and they do not necessarily cross the origin as shown. Error bars in data plots represent 95% confidence intervals calculated using the normal approximation method.

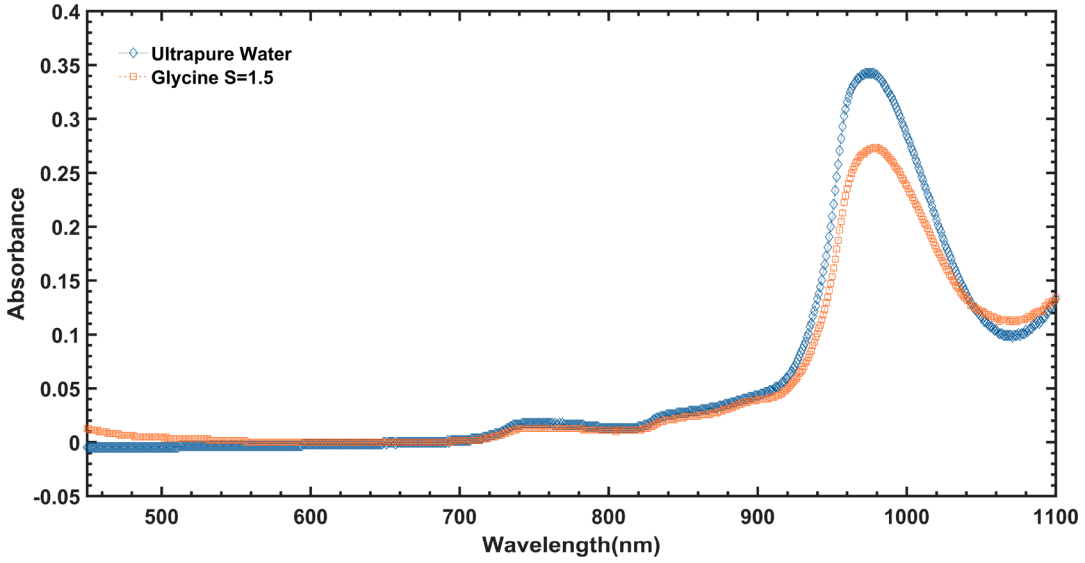

Figure 6. Vis−near-IR absorption spectra of ultrapure water and a glycine solution with $S = 1.5$. The absorbance corresponds to a beam path length of 14.6 mm.

tests, and despite achieving a higher nucleation probability (11%), they found no correlation between the binary polarization and the polymorphism of glycine.

Temperature Fluctuation and Supersaturation Change. According to classical nucleation theory, the nucleation rate exhibits a strong nonlinear behavior with respect to the supersaturation.[47,48] Therefore, minute changes in the solution temperature can alter supersaturation and lead to pronounced variations in measured induction times. Hence, it is critical to detect any spatial and temporal temperature variations during the NPLIN measurements. Most of the NPLIN studies on glycine were performed by exposing the samples to 600 laser pulses (1 min with 10 Hz repetition rate) at 1064 nm. Although the solution is considered to be transparent to the incident light, there is still a slight absorption by the solution in the near-infrared region of the spectrum, which will change both the temperature and supersaturation of the samples during the irradiation process. Furthermore, there are also reflections at the air−glass and glass−liquid interfaces as the light beam passes through the sample vials. In the following, the absorption and reflection are quantified at both 532 and 1064 nm on the basis of exposure to 1 and 600 pulses.

In order to investigate the effect of the sample heating on the nucleation probability, we ran an experiment in which the samples at two different supersaturations were exposed for 60 s to pulse trains at 10 Hz. We compared the results with those from samples irradiated by a single pulse, as shown in Figure 5 (refer to Table S6 for details). The results show that the number of laser light pulses does not dramatically alter the fraction of samples nucleated and the use of a single pulse is sufficient to trigger NPLIN. The nucleation probability after

https://dx.doi.org/10.1021/acs.cgd.0c01415
Cryst. Growth Des. 2021, 21, 631−641

Table 1. Change in Temperature and Supersaturation of Glycine Solutions Due to Energy Absorbed from 600 Pulses from Laser Radiation

supersaturation	wavelength (nm)	absorbance	absorbed energy (J) (1 pulse)	specific heat capacity (J/(g K))	density (g/cm^3)	ΔT (K) (600 pulses)	ΔS change in supersaturation after exposure to 600 pulses
1.4	532	0.043	0.030	3.44	1.096	0.60	0.017
	1064	0.112	0.227			4.52	0.118
1.5	532	0.046	0.032	3.40	1.108	0.64	0.019
	1064	0.112	0.227			4.52	0.127
1.6	532	0.042	0.030	3.36	1.120	0.59	0.019
	1064	0.112	0.227			4.52	0.136
1.7	532	0.067	0.046	3.33	1.132	0.91	0.031
	1064	0.123	0.246			4.89	0.155

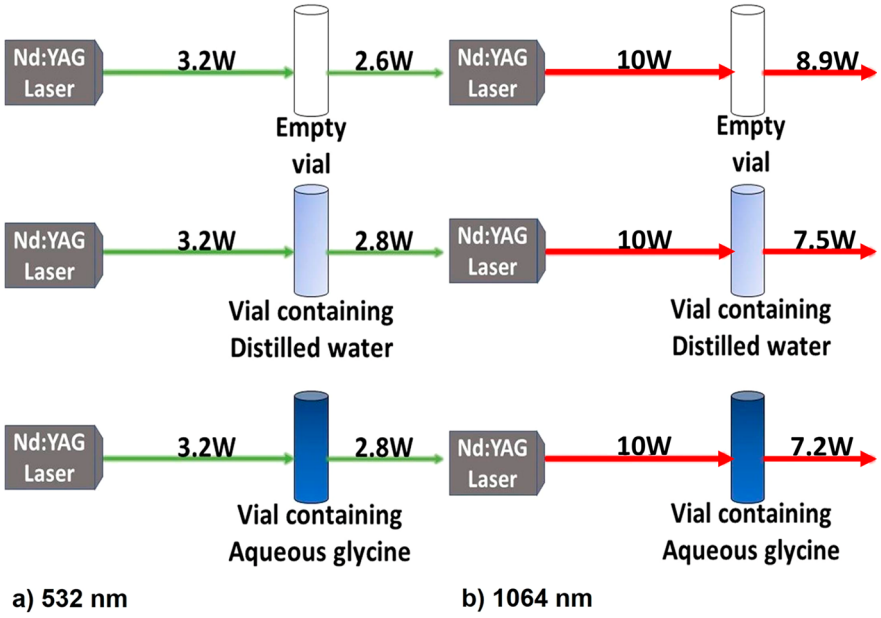

Figure 7. Quantification of energy losses (reflection and absorption) when a laser beam passes through a vial containing different substances (air, water, and glycine solution).

exposure to a large number of pulses is even somewhat lower than that caused by exposure to a single pulse, particularly evident at $S = 1.6$. This observation might be due to sample heating, lowering the prescribed supersaturation. We move further to quantify this effect by measurements of absorption, optical transmission, and solution temperature upon exposure.

Absorption of Laser Light: UV–Vis Spectra of Glycine Solutions. The absorbance of aqueous glycine solutions and ultrapure water was measured using a double-beam UV–vis spectrophotometer (Hach DR-6000). The spectrophotometer works on the principle of measuring the optical attenuation of light which passes through the sample cuvette. The absorption spectra were measured over the spectral range 450–1100 nm at a scan rate of 900 nm min^{-1}, and an example of such absorption spectra is shown in Figure 6. The spectra were corrected to eliminate optical errors caused by reflections at the surface of the 10 mm square glass cuvettes of the spectrophotometer. However, the absorbance plot in Figure 6 has been adapted to a beam path length of 14.6 mm that matches the inner diameter of our sample vials.

The energy absorbed by the glycine solutions is calculated by knowing the absorbance, which is given by

$$A = \log_{10} \frac{I_0(\lambda)}{I_T(\lambda)}$$

where A is the absorbance, $I_0(\lambda)$ is the incident intensity, and $I_T(\lambda)$ is the transmitted intensity.

By rearranging the above equation and taking the incident intensity as the sum of absorbed and transmitted intensities, we get the value of absorbed intensity (I_A) using the formula

$$I_A(\lambda) = I_0(\lambda)(1 - 10^{-A})$$

In our NPLIN experiments average powers of approximately 10 W at 1064 nm and 3.2 W at 532 nm are used at a repetition rate of 10 Hz, which correspond to energies of 1 and 0.32 J per pulse, respectively. The density of the glycine solution is determined experimentally by weighing the mass of the solution for a known volume. The procedure is repeated five times to reduce the measurement error. The specific heat capacity of aqueous glycine samples is obtained using the rule of mixtures formula,[49] which applies to solutions with multiple components. Using the specific heat capacity value in conjunction with the values for absorbance, input energy, and sample mass, the temperature increase (ΔT) is calculated with the expression

$$\Delta T = \frac{E_A}{c_p \times m}$$

https://dx.doi.org/10.1021/acs.cgd.0c01415
Cryst. Growth Des. 2021, 21, 631–641

Table 2. Summary of the Critical Experimental Parameters Used in NPLIN Studies on Glycine[a]

	our work	Liu et al.	Sun et al.	Javid et al.
polarization switching	not observed	not observed	observed	not studied; the focus was on influence of filtration
		Laser Specifications		
beam spatial profile	Gaussian	Gaussian	near top-hat	near top-hat
wavelength (nm)	1064	1064	1064	1064
repetition rate (Hz)	10	10	10	10
beam diameter (mm)	9	2.5	1.85	1
exposed volume (cm^3)	~0.705	0.045	~0.027	~0.0068
pulse duration (ns)	7	5.6	9	6
no. of pulses	1	600	600	600
intensity (GW/cm^2)	0.45	0.5	0.46	0.47
		Sample Vials		
type	borosilicate glass	Pyrex glass tubes	Pyrex glass tubes	HPLC glass vials
diameter (mm)	16.6	13	13	11
shape	cylindrical	cylindrical	cylindrical	cylindrical
total volume V_T (cm^3)	8	6	2	2
$T(V_T)$, 600 pulses (°C)	4.52	0.31	0.84	0.29
exposed volume, V_E (cm^3)	0.705	0.045	~0.027	~0.0068
$T(V_E)$, 1 pulse (°C)	0.08	0.07	0.10	0.14
V_T/V_E	11.35	133.33	74.10	294.10
		Sample Preparation		
glycine purity (%)	Sigma-Aldrich, 99.7−101	Sigma-Aldrich, 99.7−101	Plus One Pharmacia Biotech, >99.7	Sigma-Aldrich, >99%
supersaturation generation	cooling from 65 to 24 °C by natural convection	cooling from 60 to 70 to 25 °C by convection	cooling from 69 to 21 °C by convection	cooling from 60 to 25 °C by convection
filtration	no	no	no	yes
no. of samples per point and total for NPLIN at 1064 nm	100−378, ~2000	12−98, 463	40−90, 1600	50, 760

[a]All values of T were calculated using our method based on the absorbance measurements.

where E_A is the energy absorbed by the solution in J, c_p is specific heat capacity of aqueous glycine solution in J/(g K), and m is the mass of the solution per vial in g.

On the basis of the amount of energy absorbed, we then calculate how much the temperature will increase and how much the supersaturation will decrease. The change in temperature and supersaturation as well as the density, specific heat, and absorbance values are shown in Table 1.

Temperature Measurements of Solutions upon Exposure. To validate the predictions in Table 1, we measured the temperature of pure water and supersaturated glycine solutions before and after laser exposure with a thermocouple. Temperature measurements revealed that exposure to 600 pulses leads to an increase in temperature of 3−4 °C in water samples and 4−5 °C in glycine solution samples. The results in Table S7 in the Supporting Information shows that there is significant absorption at this wavelength, leading to a temperature increase (averaged over 10 samples) of 3.3 °C in an 8 mL volume of pure water and 4.5 °C in the same volume of aqueous glycine solution at $S = 1.5$. The values are in good agreement with the calculations based on the absorbance data from a UV−vis spectrophotometer.

The values in Table S7 in the Supporting Information represent the temperature of the "fully mixed" samples, although it is worth noting that a temperature gradient of about 0.5 °C/cm between the top and bottom of the vials was observed immediately after the 1 min irradiation at near-infrared wavelength. The laser was fired just at the bottom part of the vial, and the presence of this gradient leads to convection and mixing in the solution. Furthermore, measurements were carried out also at 532 nm, where only a negligible temperature increase was observed, as there is no significant absorption at this wavelength. On the basis of the temperature increase of $\Delta T = 3.3$ °C (water samples) and 4.5 °C (aqueous glycine samples) and the specific heat capacities of 4.186 J /(g K) (water) and 3.40 J/(g K) (aqueous glycine solution at $S = 1.5$), the amounts of heat absorbed from 600 laser pulses at 1064 nm are $E_A = c_p \times m \times \Delta T = 110$ and 136 J, respectively.

Optical Transmission Measurements. Apart from absorption, some of the laser light energy is lost by reflection off the walls of the cylindrical borosilicate glass vial due to a change in the refractive index at the air−glass and glass−air interfaces. The reduction in laser energy caused by both reflection and absorption was measured at both 532 and 1064 nm using input powers of 3.2 and 10 W, respectively, as shown in Figure 7. In an empty vial, the laser beam passes twice through its glass walls, striking four air−glass or glass−air interfaces, and the amount of reflections is nearly equal at each of them. For example, at 1064 nm, each interface contributes by 0.275 W to a total power loss of 1.1 W due to reflections. When a solution is placed in the vial, the number of interfaces is reduced from 4 to 2 due to the smaller difference between the refractive indices of the glass and solution. At 1064 nm, the refractive index of borosilicate glass is 1.5, while that of the glycine solution of $S = 1.5$ is estimated as 1.4;[38,50] therefore, the reflection losses at the glass−solution interface are negligible ($R \approx 0.1\%$). This becomes obvious from the power measurements at 532 nm, shown in Figure 7a, where an increase in exit power is obtained when the glass vial is filled with water or glycine solution. The same would occur also at 1064 nm, but the output power enhancement is hindered by the solution's absorption of laser photons at this wavelength.

https://dx.doi.org/10.1021/acs.cgd.0c01415
Cryst. Growth Des. 2021, 21, 631−641

When a vial containing water is exposed to infrared light, the power absorbed is 1.95 W, while the loss by reflections is reduced to 0.55 W. The total energy absorbed is 0.195 J/pulse and 117 J after exposure to 600 pulses. In the case of a glycine solution of S = 1.5, the absorption losses account for 0.225 J/pulse and 135 J (600 pulses). The analysis of the laser energy by reflection and absorption is consistent with both the calculated and measured temperature increase in the sample vials. Thus, the temperature effects can explain the lower nucleation fractions observed in solutions irradiated with 600 pulses, as seen in Figure 5. There are two competing phenomena that can affect the nucleation rate. The reduction in supersaturation due to a temperature increase causes a decrease in the nucleation rate, while the mixing induced by the temperature gradient will lead to an increase in the growth rate and hence the measured induction time measured will decrease. The fact that the probability of nucleation is somewhat lower when 600 pulses are used suggests that a reduction in supersaturation may have a stronger effect than the enhanced growth due to convective mixing. Hence, the use of trains of pulses can have a clear temperature effect and should be avoided when large irradiated volumes are used in order not to disturb the measurements.

Finally, we discuss our results on circularly and linearly polarized light given in Figure 4 in the context of previous reports in the literature. It is important to note that nucleation is a highly stochastic process and the polymorph crystallizing from solution in NPLIN experiments can be influenced by various experimental factors such as ambient and local temperature, supersaturation, chemical purity, exposed volume, laser polarization, and energy density. Despite significant efforts to maintain these factors as consistently as possible, minor variations in any of them can alter the outcome. This situation makes the reproducibility of NPLIN experiments on polymorphism rather challenging.

Sample Heating. In terms of the temperature control, the NPLIN studies on nucleation of aqueous glycine solutions at near-IR wavelengths can be performed using a tradeoff between the number of laser pulses and the irradiated volume of the sample. To facilitate a discussion as to why this might be the case, we provide a table comparing the critical experimental parameters in NPLIN experiments with glycine (Table 2). We chose to irradiate our samples with a large laser beam diameter (9 mm) in order to enhance the nucleation probability through a large exposed volume (V_E). In addition, we employed only a single laser pulse in order to avoid the heating effects caused by both the solution's absorption of light photons and the low ratio of the "total sample volume" to the "exposed volume" (V_T/V_E). Our temperature measurements indicate that a large number of pulses (600) increases the temperature of the solution up to 4−5 °C. Hence, the samples are inadvertently heated and supersaturation is lowered during the exposure.

In contrast, the previous studies on the nucleation of glycine involved small beam diameters (1−2 mm, presumably to keep the bulk temperature stable through a large V_T/V_E ratio), although a smaller irradiation region is expected to be less favorable in terms of nucleation probability. Nevertheless, the temperature of the sample along the laser beam path could increase significantly when 600 pulses are used. That would trigger a mass transfer by natural convection, thus increasing the overall irradiated volume and boosting the growth rate and hence the apparent nucleation rate/probability. The apparent nucleation rate is calculated by the measured induction time, a parameter influenced by both nucleation and growth. That might be the reason our nucleation fraction is not higher than those from previous reports (Figure 1a of ref 37) despite the use of a larger beam diameter.

Quality of Polarization. As shown in Figure 4, the type of polymorph in the NPLIN of glycine is not biased by the laser polarization. This result agrees with Liu et al.,[38] yet it contradicts the earlier reports by Garetz et al.[12] and Sun et al.[13] Next, we briefly discuss the possible effect of the quality of polarization on the polymorphism of glycine, as limited efforts have been made in this regard. Sun et al. were the only ones who showed that, within the polarization switching window, the type of polymorph produced is strongly influenced by the degree of polarization of the laser light. They investigated the dependence of glycine polymorph formation on the ellipticity of the IR laser radiation at supersaturation S = 1.45−1.55 and observed that the ellipticity range of e = 0−0.9 generated only γ-glycine, while the range e = 0.9−1 generated only α-glycine (Figure 4 of ref 13). We note that the ellipticity e is the ratio of the semiminor to semimajor axis of a polarization ellipse described by the electric field vector of the laser light; it varies from e = 0 for linear polarization to e = 1 for circular polarization. The results revealed that α-glycine in particular is highly sensitive to the ellipticity parameter and a slight deviation from a nearly perfect circular polarization could hamper its production. Therefore, a careful quantification of the polarization quality in the NPLIN experiments needs further investigation.

Sample Preparation Procedure. Aging is an experimental parameter that is commonly considered to influence crystallization.[51] A supersaturated solution cooled with different temperature profiles can produce different polymorphs. As a rule of thumb, fast-cooled samples give rise to metastable polymorphs whereas slower cooling rates produce stable polymorphs. However, all of the studies considered in Table 2 have very similar aging procedures, and so we can not attribute the different results on polarization switching to aging effects.

Purity and Seeding. Boldyreva et al.[32] claim that the likelihood of one particular glycine polymorph (e.g., γ) crystallizing from a pure aqueous solution depends on the presence of the seeds of that polymorph in the commercial powder used for preparing the supersaturated solution. The fact that the chemical compounds sold (by various suppliers or by the same supplier but from different batches) normally differ in the α-/γ-polymorph ratio could be the reason some results of experiments on crystallization of glycine are not reproducible. For example, although the glycine compound used in our study was purchased from the same supplier as was used by Liu et al., structural analysis revealed that our as-purchased solid was α-glycine while theirs was a mixture of α- and γ-polymorphs. Despite this difference in the form of starting material, our results on polarization switching agree with those of Liu et al.[38] The polarization-switching effect is reportedly occurring over a narrow range of supersaturations and is dependent on the solution temperature as well as the wavelength and intensity of the laser. Its existence still remains under controversy, but an impartial observation requires identical experimental conditions and careful monitoring of the control parameters, particularly impurities—an experimental challenge for future studies.

https://dx.doi.org/10.1021/acs.cgd.0c01415
Cryst. Growth Des. 2021, 21, 631−641

CONCLUSIONS

We have investigated the influence of laser light excitation properties (number of pulses, type of polarization) on the kinetics of glycine nucleation and glycine's polymorphic form in aqueous solutions using overall more than 1000 samples for improved statistical significance. Our results showed that laser irradiation enhances the nucleation rate in comparison to spontaneous nucleation and nucleation via crash-cooling by reducing the induction times from days to hours. In terms of polymorph control, the direct nucleation of γ-glycine, which can be obtained using crash-cooling at high supersaturation values, is already obtained at much lower supersaturations using NPLIN. In addition, NPLIN favors a steeper transition between the two polymorphs ($\alpha \rightarrow \gamma$) in comparison to the crash-cooling method or other nucleation methods studied previously. The linear and circular polarization of the laser light did not reproduce the polarization-switching effect observed by Garetz et al., our results being in the line with those reported by Liu et al.

In our experiments, the NPLIN probability at 1064 nm is not affected significantly by the number of laser pulses; a single pulse proved capable of triggering nucleation even with a slightly higher efficiency in comparison to irradiation by multiple pulses that are often employed in laser-assisted nucleation studies. We rationalize this observation on the basis of the ability of aqueous solutions to absorb light at near-infrared wavelengths. An analysis of the heating effects in the glycine samples when multiple pulses were used was performed by measuring the reflection and transmission of light at the sample interfaces as well as recording the absorption spectra of the solution. The results showed that the temperature of the samples increases by at least 4 °C during exposure, leading to a drop in supersaturation by 0.15, and thus lowering the nucleation rate. The temperature effects should be avoided, and their extent is usually lowered by reducing the volume of the solution exposed to laser radiation. However, a small exposed volume can in turn affect the nucleation probability. We hope the presented results and discussion contribute to efforts to establish a complete mechanistic understanding of NPLIN of glycine from aqueous solutions.

ASSOCIATED CONTENT

Supporting Information

The Supporting Information is available free of charge at https://pubs.acs.org/doi/10.1021/acs.cgd.0c01415.

Shape of a laser beam propagating through a cylindrical sample vial, the time-dependent temperature profile of the crash-cooled samples, and tables of additional data (PDF)

AUTHOR INFORMATION

Corresponding Author

Huseyin Burak Eral − *Intensified Reaction & Separation Systems, Process & Energy Laboratory, Delft University of Technology, 2628 CB Delft, The Netherlands;* orcid.org/0000-0003-3193-452X; Email: h.b.eral@tudelft.nl

Authors

Daniel Irimia − *Intensified Reaction & Separation Systems, Process & Energy Laboratory, Delft University of Technology, 2628 CB Delft, The Netherlands;* orcid.org/0000-0001-6131-6912

Jenkins Jose Shirley − *Intensified Reaction & Separation Systems, Process & Energy Laboratory, Delft University of Technology, 2628 CB Delft, The Netherlands*

Anshul S. Garg − *Intensified Reaction & Separation Systems, Process & Energy Laboratory, Delft University of Technology, 2628 CB Delft, The Netherlands*

Davey P.A. Nijland − *Intensified Reaction & Separation Systems, Process & Energy Laboratory, Delft University of Technology, 2628 CB Delft, The Netherlands*

Antoine E. D. M. van der Heijden − *Intensified Reaction & Separation Systems, Process & Energy Laboratory, Delft University of Technology, 2628 CB Delft, The Netherlands*

Herman J. M. Kramer − *Intensified Reaction & Separation Systems, Process & Energy Laboratory, Delft University of Technology, 2628 CB Delft, The Netherlands;* orcid.org/0000-0003-3580-8432

Complete contact information is available at: https://pubs.acs.org/10.1021/acs.cgd.0c01415

Author Contributions

The manuscript was written through contributions of all authors. All authors have given approval to the final version of the manuscript.

Funding

This work is part of the research program open technology scheme with project number 16714, which is financed by the Dutch Research Council (NWO).

Notes

The authors declare no competing financial interest.

REFERENCES

(1) Garetz, B. A.; Aber, J. E.; Goddard, N. L.; Young, R. G.; Myerson, A. S. Nonphotochemical, Polarization-Dependent, Laser-Induced Nucleation in Supersaturated Aqueous Urea Solutions. *Phys. Rev. Lett.* **1996**, *77*, 3475−3476.

(2) Virone, C.; Kramer, H. J. M.; Van Rosmalen, G. M.; Stoop, A. H.; Bakker, T. W. Primary nucleation induced by ultrasonic cavitation. *J. Cryst. Growth* **2006**, *294*, 9−15.

(3) Lakerveld, R.; Verzijden, N. G.; Kramer, H. J. M.; Jansens, P. Application of Ultrasound for Start-Up of Evaporative Batch Crystallization of Ammonium Sulfate in a 75-L Crystallizer. *AIChE J.* **2011**, *57*, 3367−3377.

(4) Radacsi, N.; ter Horst, J. H.; Stefanidis, G. D. Microwave-Assisted Evaporative Crystallization of Niflumic Acid for Particle Size Reduction. *Cryst. Growth Des.* **2013**, *13*, 4186−4189.

(5) Kacker, R.; Salvador, P. M.; Sturm, G. S. J.; Stefanidis, G. D.; Lakerveld, R.; Nagy, Z. K.; Kramer, H. J. M. Microwave Assisted Direct Nucleation Control for Batch Crystallization: Crystal Size Control with Reduced Batch Time. *Cryst. Growth Des.* **2016**, *16*, 440−446.

(6) Kacker, R.; Radoiu, M.; Kramer, H. J. M. Novel Design Integrating a Microwave Applicator into a Crystallizer for Rapid Temperature Cycling. A Direct Nucleation Control Study. *Cryst. Growth Des.* **2017**, *17*, 3766−3774.

(7) Yuyama, K.; Sugiyama, T.; Masuhara, H. Millimeter-Scale Dense Liquid Droplet Formation and Crystallization in Glycine Solution Induced by Photon Pressure. *J. Phys. Chem. Lett.* **2010**, *1*, 1321−1325.

(8) Yuyama, K.; Sugiyama, T.; Masuhara, H. Laser Trapping and Crystallization Dynamics of L-Phenylalanine at Solution Surface. *J. Phys. Chem. Lett.* **2013**, *4*, 2436−2440.

(9) Iwakura, I.; Komori-Orisaku, K.; Hashimoto, S.; Akai, S.; Kimura, K.; Yabushita, A. Formation of thioglucoside single crystals by coherent molecular vibrational excitation using a 10-fs laser pulse. *Communications Chemistry* **2020**, *3*, 35.

(10) Lee, S.; Evans, J. M. B.; Erdemir, D.; Lee, A. Y.; Garetz, B. A.; Myerson, A. S. Nonphotochemical Laser Induced Nucleation of Hen Egg White Lysozyme Crystals. *Cryst. Growth Des.* **2008**, *8*, 4255−4261.
(11) Matic, J.; Sun, X.; Garetz, B. A.; Myerson, A. S. Intensity, Wavelength, and Polarization Dependence of Nonphotochemical Laser-Induced Nucleation in Supersaturated Aqueous Urea Solutions. *Cryst. Growth Des.* **2005**, *5*, 1565−1567.
(12) Garetz, B. A.; Matic, J.; Myerson, A. S. Polarization Switching of Crystal Structure in the Nonphotochemical Light-Induced Nucleation of Supersaturated Aqueous Glycine Solutions. *Phys. Rev. Lett.* **2002**, *89*, 175501.
(13) Sun, X.; Garetz, B. A.; Myerson, A. S. Supersaturation and Polarization Dependence of Polymorph Control in the Non-photochemical Laser-Induced Nucleation (NPLIN) of Aqueous Glycine Solutions. *Cryst. Growth Des.* **2006**, *6*, 684−689.
(14) Kacker, R.; Dhingra, S.; Irimia, D.; Ghatkesar, M. K.; Stankiewicz, A. I.; Kramer, H. J. M.; Eral, H. B. Multiparameter Investigation of Laser-Induced Nucleation of Supersaturated Aqueous KCl Solutions. *Cryst. Growth Des.* **2018**, *18*, 312−317.
(15) Barber, E. R.; Kinney, N. L. H.; Alexander, A. J. Pulsed laser-induced nucleation of sodium chlorate at high energy densities. *Cryst. Growth Des.* **2019**, *19*, 7106−7111.
(16) Alexander, A. J.; Camp, P. J. Single Pulse, Single Crystal Laser-Induced Nucleation of Potassium Chloride. *Cryst. Growth Des.* **2009**, *9*, 958−963.
(17) Sugiyama, T.; Adachi, T.; Masuhara, H. Crystallization of Glycine by Photon Pressure of a Focused CW Laser Beam. *Chem. Lett.* **2007**, *36*, 1480−1481.
(18) Alexander, A. J.; Camp, P. J. Non-photochemical laser-induced nucleation. *J. Chem. Phys.* **2019**, *150*, 040901.
(19) Oxtoby, D. W. Crystals in a flash. *Nature* **2002**, *420*, 277.
(20) Knott, B. C.; Doherty, M. F.; Peters, B. A simulation test of the optical Kerr mechanism for laser-induced nucleation. *J. Chem. Phys.* **2011**, *134*, 154501.
(21) Warshavsky, V. B.; Shchekin, A. K. The effects of external electric field in thermodynamics of formation of dielectric droplet. *Colloids Surf., A* **1999**, *148*, 283−290.
(22) Isard, J. O. Calculation of the influence of an electric field on the free energy of formation of a nucleus. *Philos. Mag.* **1977**, *35*, 817.
(23) Mirsaleh-Kohan, N.; Fischer, A.; Graves, B.; Bolorizadeh, M.; Kondepudi, D.; Compton, R. N. Laser Shock Wave Induced Crystallization. *Cryst. Growth Des.* **2017**, *17*, 576−581.
(24) Soare, A.; Dijkink, R.; Rodriguez Pascual, M.; Sun, C.; Cains, P. W.; Lohse, D.; Stankiewicz, A. I.; Kramer, H. J. M. Crystal Nucleation by Laser-Induced Cavitation. *Cryst. Growth Des.* **2011**, *11*, 2311−2316.
(25) Jacob, J. A.; Sorgues, S.; Dazzi, A.; Mostafavi, M.; Belloni, J. Homogeneous Nucleation-Growth Dynamics Induced by Single Laser Pulse in Supersaturated Solutions. *Cryst. Growth Des.* **2012**, *12*, 5980−5985.
(26) Jose-Shirley, J. *NPLIN and LIN: A study into the mechanism*; TU Delft: 2020; http://repository.tudelft.nl/.
(27) Sindt, J. O.; Alexander, A. J.; Camp, P. J. Effects of nanoparticle heating on the structure of a concentrated aqueous salt solution. *J. Chem. Phys.* **2017**, *147*, 214506.
(28) McEwan, K. J.; Madden, P. A. Transient grating effects in absorbing colloidal suspensions. *J. Chem. Phys.* **1992**, *97*, 8748.
(29) Lowen, H.; Madden, P. A. A microscopic mechanism for shockwave generation in pulsed-laser-heated colloidal suspensions. *J. Chem. Phys.* **1992**, *97*, 8760.
(30) Jawor-Baczynska, A.; Sefcik, J.; Moore, B. D. 250 nm Glycine-Rich Nanodroplets Are Formed on Dissolution of Glycine Crystals But Are Too Small To Provide Productive Nucleation Sites. *Cryst. Growth Des.* **2013**, *13*, 470−478.
(31) Ward, M. R.; Mackenzie, A. M.; Alexander, A. J. Role of Impurity Nanoparticles in Laser-Induced Nucleation of Ammonium Chloride. *Cryst. Growth Des.* **2016**, *16*, 6790−6796.
(32) Boldyreva, E. V.; Drebushchak, V. A.; Drebushchak, T. N.; Paukov, I. E.; Kovalevskaya, Y. A.; Shutova, E. S. POLYMORPHISM OF GLYCINE. Thermodynamic aspects. Part I. Relative stability of the polymorphs. *J. Therm. Anal. Calorim.* **2003**, *73*, 409−418.
(33) Llinàs, A.; Goodman, J. M. Polymorph control: past, present and future. *Drug Discovery Today* **2008**, *13*, 198−210.
(34) Mangin, D.; Puel, F.; Veesler, S. Polymorphism in Processes of Crystallization in Solution: A Practical Review. *Org. Process Res. Dev.* **2009**, *13*, 1241−1253.
(35) Nicoud, L.; Licordari, F.; Myerson, A. S. Polymorph control in batch seeded crystallizers. A case study with paracetamol. *CrystEngComm* **2019**, *21*, 2105−2118.
(36) Kitamura, M. Strategy for control of crystallization of polymorphs. *CrystEngComm* **2009**, *11*, 949−964.
(37) Zaccaro, J.; Matic, J.; Myerson, A. S.; Garetz, B. A. Nonphotochemical, Laser-Induced Nucleation of Supersaturated Aqueous Glycine Produces Unexpected ç-Polymorph. *Cryst. Growth Des.* **2001**, *1*, 5−8.
(38) Liu, Y.; van den Berg, M. H.; Alexander, A. J. Supersaturation dependence of glycine polymorphism using laser-induced nucleation, sonocrystallization and nucleation by mechanical shock. *Phys. Chem. Chem. Phys.* **2017**, *19*, 19386.
(39) Ikni, A.; Clair, B.; Scouflaire, P.; Veesler, S.; Gillet, J. M.; El Hassan, N.; Dumas, F.; Spasojević-de Biré, A. Experimental Demonstration of the Carbamazepine Crystallization from Non-photochemical Laser-Induced Nucleation in Acetonitrile and Methanol. *Cryst. Growth Des.* **2014**, *14*, 3286−3299.
(40) Sun, X.; Garetz, B. A.; Myerson, A. S. Polarization Switching of Crystal Structure in the Nonphotochemical Laser-Induced Nucleation of Supersaturated Aqueous L-Histidine. *Cryst. Growth Des.* **2008**, *8*, 1720−1722.
(41) Li, W.; Ikni, A.; Scouflaire, P.; Shi, X.; El Hassan, N.; Gémeiner, P.; Gillet, J. M.; Spasojević-de Biré, A. Non-Photochemical Laser-Induced Nucleation of Sulfathiazole in a Water/Ethanol Mixture. *Cryst. Growth Des.* **2016**, *16*, 2514−2526.
(42) Javid, N.; Kendall, T.; Burns, I. S.; Sefcik, J. Filtration Suppresses Laser-Induced Nucleation of Glycine in Aqueous Solutions. *Cryst. Growth Des.* **2016**, *16*, 4196−4202.
(43) Park, K.; Evans, J. M. B.; Myerson, A. S. Determination of Solubility of Polymorphs Using Differential Scanning Calorimetry. *Cryst. Growth Des.* **2003**, *3*, 991−995.
(44) Yang, X.; Wang, X.; Ching, C. B. Solubility of Form α and Form γ of Glycine in Aqueous Solutions. *J. Chem. Eng. Data* **2008**, *53*, 1133−1137.
(45) Dalton, J. B.; Schmidt, C. L. A. The solubilities of certain amino acids in water, the densities of their solutions at twenty-five degrees and the calculated heats of solution and partial molar volumes. *J. Biol. Chem.* **1933**, *103*, 549−578.
(46) Boldyreva, E. V.; Drebushchak, V. A.; Drebushchak, T. N.; Paukov, I. E.; Kovalevskaya, Y. A.; Shutova, E. S. POLYMORPHISM OF GLYCINE. Thermodynamic aspects. Part II. Polymorphic transitions. *J. Therm. Anal. Calorim.* **2003**, *73*, 419−428.
(47) Lewis, A.; Seckler, M.; Kramer, H.; van Rosmalen, G. *Industrial Crystallization: Fundamentals and Applications*; Cambridge University Press: 2015.
(48) Myerson, A. S.; Erdemir, D.; Lee, A. Y. *Handbook of Industrial Crystallization*; Cambridge University Press: 2019.
(49) Rule of mixtures for specific heat capacity/Thermtest Instruments: https://thermtest.com/rule-of-mixtures-calculator.
(50) Soto, A.; Arce, A.; Khoshkbarchi, M. K. Effect of cation and anion of an electrolyte on apparent molar volume, isentropic compressibility and refractive index of glycine in aqueous solutions. *Biophys. Chem.* **1999**, *76*, 73−82.
(51) Hua, T.; Valentín-Valentín, C.; Gowayed, O.; Lee, S.; Garetz, B. A.; Hartman, R. L. Microfluidic Laser-Induced Nucleation of Supersaturated Aqueous Glycine Solutions. *Cryst. Growth Des.* **2020**, *20*, 6502−6509.

https://dx.doi.org/10.1021/acs.cgd.0c01415
Cryst. Growth Des. 2021, 21, 631−641